

1 **Flow cytometry and machine learning enable identification of allergenic urban tree pollen.**

2 Authors : Sarah Tardif<sup>1,2</sup>, Maria Raquel Kanieski<sup>4</sup>, Gauthier Lapa<sup>1,2</sup>, Grégoire Bonnamour<sup>1,3</sup>, Rita Sousa-  
3 Silva<sup>5</sup>, Isabelle Laforest-Lapointe<sup>2,6</sup>, Alain Paquette<sup>1,2</sup>

4  
5 <sup>1</sup> Département des sciences biologiques, Université du Québec à Montréal, Montréal, QC, Canada.

6 <sup>2</sup> Centre for Forest Research, Université du Québec à Montréal, Montréal, QC, Canada.

7 <sup>3</sup>Centre d'excellence en recherche sur les maladies orphelines-Fondation Courtois (CERMO-FC),  
8 Université du Québec à Montréal, Montréal, QC, Canada.

9 <sup>4</sup> Universidade do Estado de Santa Catarina, Depto. Engenharia Florestal, Lages, SC, Brasil.

10 <sup>5</sup> Institute of Environmental Sciences, Department of Environmental Biology, Leiden University, Leiden,  
11 The Netherlands.

12 <sup>6</sup> Département de Biologie, Université de Sherbrooke, Sherbrooke, QC, Canada.

13 *Correspondence to:* Sarah Tardif (sarahtardif02@gmail.com)

14 **Abstract**

15 Exposure to allergenic pollen is a major public health concern, as it is a key trigger for respiratory allergies,  
16 including seasonal allergic rhinitis, which affects approximately 20% of the global population. Monitoring  
17 airborne pollen is essential for prevention and clinical management, yet traditional identification methods,  
18 such as light microscopy, are time-consuming and often limited to genus- or family-level resolution. Here,  
19 we present a high-throughput approach combining flow cytometry with machine learning to identify pollen  
20 from urban environments. We collected a reference database of pollen from 97 species across 34 genera,  
21 representing the dominant allergenic trees and other common airborne taxa in Montreal, Canada. Using  
22 flow cytometry, we measured particle size, granularity, and fluorescence intensity across multiple excitation  
23 and emission channels, and applied a Random Forest classifier to distinguish pollen taxa. At the species  
24 level, the model achieved a mean  $F_1$ -score of 0.76, while genus-level classification reached 0.90, with  
25 misclassifications largely occurring among closely related species. Granularity and fluorescence parameters  
26 from the violet and blue lasers were the most distinctive features. Our results demonstrate that flow  
27 cytometry combined with machine learning provides an efficient, scalable alternative to microscopy, with  
28 potential for large-scale urban pollen monitoring.

## 29 **1 Introduction**

30 Exposure to allergenic pollen is a major public health concern, as it is a key risk factor for respiratory  
31 allergies. Seasonal allergic rhinitis affects approximately 20 % of the global population (Savouré et al.,  
32 2022) and is expected to worsen with climate change, which is projected to lengthen pollen seasons  
33 (Anderegg et al., 2021; Mousavi et al., 2024; Zhang and Steiner, 2022; Ziska et al., 2019). Rising  
34 temperatures and CO<sub>2</sub> levels stimulate plant growth, increasing pollen levels (Kim et al., 2018; Ladeau and  
35 Clark, 2006) and the allergenicity of pollen grains (Ahlholm et al., 1998; Kim et al., 2018). For allergy  
36 sufferers and healthcare providers, reliable pollen information, including which plant species and pollen  
37 traits contribute to different allergenicity properties, is essential for prevention and effective treatment, but  
38 remains scarce (Dunker et al., 2022; Medek et al., 2025; Sousa-Silva et al., 2020).

39 Expanding pollen monitoring networks in urban areas, which host most of the world's population, is  
40 increasingly recognized as essential (Tummon et al., 2024), yet this also requires processing a large number  
41 of pollen samples and thus highlights a clear need for efficient, accurate, and high temporal resolution  
42 identification methods. Over the past decades, several analytical techniques have been developed for pollen  
43 detection and classification, each having advantages and limitations. Light microscopy remains the standard  
44 method used worldwide for pollen identification, but it is time-consuming and requires highly trained  
45 specialists (Brennan et al., 2019; Dunker et al., 2021, 2022; Gierlicka et al., 2022; de Weger et al., 2013).  
46 Although pollen morphology, defined by size, shape, apertures, and texture (Ogden et al., 1974; Smith,  
47 1984), supports taxonomic identification, subtle interspecific differences restrict identification to genus or  
48 family level in most cases. Automated slide scanning, sometimes coupled with a machine learning  
49 algorithm, has improved efficiency but still faces limitations in distinguishing species from the same genus  
50 or family (Dunker et al., 2021; Holt and Bennett, 2014). Advanced imaging techniques, such as scanning  
51 electron microscopy (SEM), transmission electron microscopy (TEM), and optical diffraction tomography  
52 (ODT), provide much higher resolution for detailed analysis of pollen structures, but are costly or  
53 impractical for large-scale monitoring (Gierlicka et al., 2022). Molecular biology techniques, particularly  
54 metabarcoding and PCR-based methods, have the potential to enable species-level identification yet face  
55 challenges such as high costs, the presence of DNA inhibitors that can limit sensitivity and cause false  
56 negative, the limitations of taxonomic resolution, and the inability to quantify pollen abundance (Dunker et  
57 al., 2021; Gierlicka et al., 2022).

58 More recently, fluorescence spectroscopy and flow cytometry have emerged as promising approaches  
59 (Gierlicka et al., 2022; Šaulienė et al., 2019). These methods are based on the size and autofluorescence  
60 properties of particles, such as the pollen grains, and when combined with holographic images and machine

61 or deep learning, they can improve classification accuracy and enable automated (Dunker et al., 2022; Erb  
62 et al., 2024; Sikoparija et al., 2024; Swanson et al., 2023) and high-throughput identification ( $\approx 5000$  grains  
63  $s^{-1}$ ) (Dunker et al., 2021; Gierlicka et al., 2022). Because each species has a specific fluorescence and  
64 granularity signature, it is possible to distinguish even morphologically similar taxa (Dunker et al., 2021).

65 Our study aims to develop a classification model capable of identifying pollen from urban environments at  
66 species and genus levels. Here we present the necessary first step in the development of a broader  
67 methodological pipeline for the analysis of airborne pollen. We built a reference collection representing the  
68 main tree species found across the city of Montreal, Canada. Unlike previous studies that rely on  
69 microscopic or imaging data, our approach relies exclusively on flow cytometry measurements, i.e.  
70 fluorescence intensity, particle size, and granularity to characterize pollen. This choice is motivated by the  
71 fact that most cytometers routinely used in healthcare and clinical settings are limited to these parameters.  
72 Consequently, developing a model based on these features enhances its applicability and ensures  
73 compatibility with the most widely implemented cytometry platforms. We then evaluated the performance  
74 of the machine-learning classification model trained on these flow cytometry parameters and identified  
75 those that contribute most to differentiating pollen species and genera.

## 76 **2 Methodology**

### 77 **2.1 Pollen collection**

78 To train the machine learning classification model, we created a reference database of pollen grains collected  
79 directly from plants of known species (mostly trees). The reference collection included pollen from both  
80 common urban tree species as well as widely planted hybrid cultivars.

81 Tree species were selected based on three criteria: (1) their relative abundance on the Island of Montreal,  
82 ensuring representation of the dominant urban taxa; (2) their anemophilous nature, since wind-pollinated  
83 species are typically the most allergenic (D'Amato et al., 2007; Falagiani, 1989); and (3) the inclusion of  
84 multiple species within each genus, to enable species-level discrimination where possible. Other species  
85 such as from the Rosaceae family were also included to increase resolution. For each selected species, pollen  
86 was collected from three individual trees from the Montreal Botanical Garden (for ease of identification) or  
87 among public trees across the city. At flowering time, ten floral units (flowers, catkins or male cones) were  
88 collected per tree, sampling different parts of the crown to capture intra-individual variation among pollen  
89 grains. We also included pollen from the Poaceae family (grasses) and the genus *Ambrosia* (ragweed), given  
90 their well-known allergenic potential (D'Amato et al., 2007; Falagiani, 1989). Their inclusion enabled the  
91 model to learn to discriminate tree pollen from other common airborne particle types, as real-world

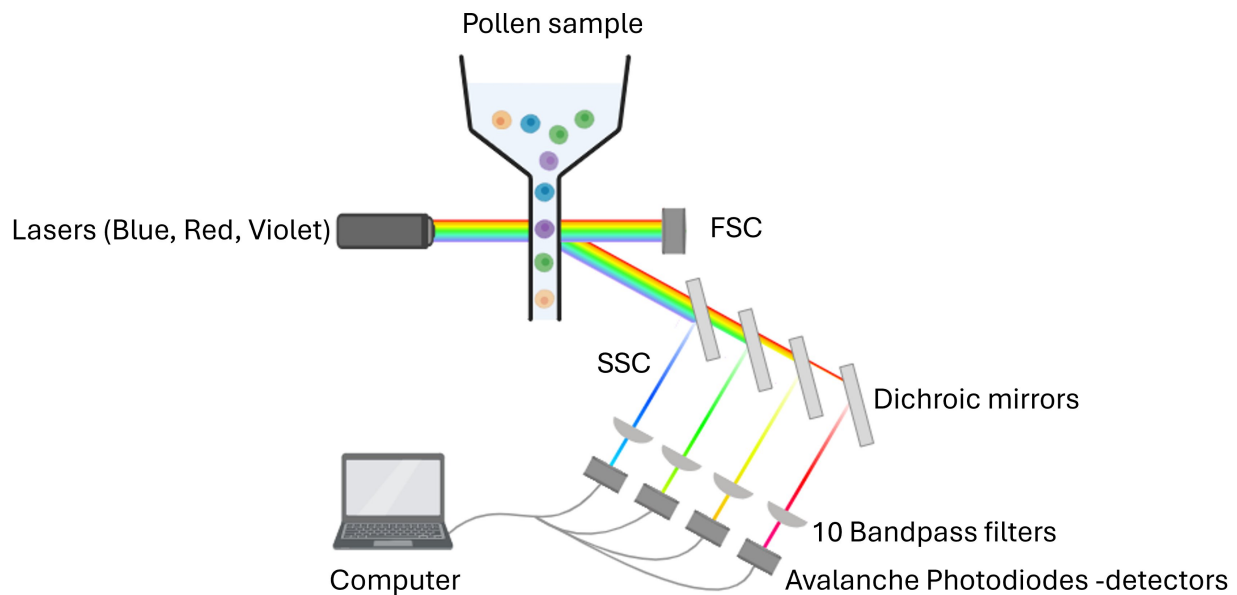
92 environmental samples typically comprise a heterogeneous mix of tree, grass, and weed pollen, along with  
93 various non-pollen particulates. In the laboratory, floral units were placed in pre-labelled paper bags with  
94 desiccant gel. Pollen was extracted from the floral units using a filtration system that retained only particles  
95 between 5 and 100  $\mu\text{m}$  in diameter, a size range that includes pollen grains but also particles of similar size.  
96 Filtration also prevents clogging of the flow cytometer because, as is generally recommended, particles  
97 should not exceed one-third to one-fifth of the width of the flow cell, which limits particle size to  
98 approximately 100  $\mu\text{m}$  on the CytoFLEX instrument we used. The filtrate was then suspended in Dulbecco's  
99 phosphate-buffered saline (PBS) solution, a standard neutral isotonic buffer commonly used in flow  
100 cytometry to minimize aggregation (Aloisi et al., 2015; Dunker et al., 2021b) (see detailed protocol in the  
101 supplementary material). A subsample was examined under a light microscope to confirm the presence of  
102 pollen grains. If pollen was present, the sample was retained; if not, sampling was repeated, including  
103 filtration, and if necessary, additional flowers were collected.

104

## 105 **2.2 Flow cytometry**

106 Each pollen sample was analysed using flow cytometry (Fig. 1). Measurements were performed with a  
107 CytoFLEX cytometer (Beckam Coulter, Inc.), equipped with three excitation lasers at wavelengths of 405  
108 nm (violet), 488 nm (blue), and 640 nm (red). Due to a hydrodynamic flow stream, each pollen grain passes  
109 sequentially through each laser, which excites fluorescent phenolic compounds present in the sporopollenin  
110 of the pollen grain's outer wall. Depending on their peptide composition, these fluorophores absorb light at  
111 a certain wavelength and emit light radiation at a different wavelength in return producing a characteristic  
112 fluorescence signature that varies among species. For each laser, avalanche photodiode (APD) detectors  
113 measure the intensity of light emitted at different wavelengths using ten filters: 450/45, 525/40, 610/20  
114 (violet laser), 525/40, 585/42, 690/50, 780/60 (blue laser), 660/10, 712/25, 780/60 nm (red laser). Each filter  
115 value, such as 450/45, follows a simple convention: the first value corresponds to the central wavelength  
116 (in nanometers, nm), which is the midpoint of the light allowed to pass through the filter; the second  
117 corresponds to the bandwidth, i.e., the width of this "window" of light. Thus, a 450/45 filter transmits light  
118 between 427.5 nm and 472.5 nm (i.e.,  $450 \pm 22.5$  nm). In addition to fluorescence, two scatter parameters  
119 were recorded to describe particle morphology: grain size and granularity. The forward scatter (FSC) detects  
120 light scattered at low angles in the forward direction, which correlates with the cross-sectional area of the  
121 particle, equivalent to a spherical diameter. For non-spherical particles like pollen (prolate, oblate,  
122 tricolporate, etc.), FSC reflects an average optical cross-section as the particle passes through the laser in a  
123 random orientation. The sideways scatter (SSC) detects light scattered at  $\sim 90^\circ$  (orthogonal) to the laser  
124 beam, which is sensitive to internal complexity and surface irregularities. In pollen, this captures internal

125 granularity, wall sculpturing, apertures, vacuoles/ pollen sacs. The more complex the structure and texture  
126 of the pollen grain, the higher the granularity values will be.



127  
128 **Figure 1:** Flow cytometry workflow on the CytoFLEX (Beckman Coulter, Inc.). Sample containing pollen  
129 enters at the top, and then is excited by three lasers in the blue ( $\lambda=488\text{nm}$ ), red ( $\lambda=640\text{nm}$ ) and violet  
130 ( $\lambda=405\text{nm}$ ) wavelengths, 10 dichroic mirrors, bandpass filters and detectors in different wavelength ranges  
131 ( $\lambda=450/45, 525/40, 610/20, 585/42, 525/40, 690/50, 780/60, 660/10, 712/25$  and  $780/60$  nm). There are two  
132 additional detectors for size and granularity: forward scatter (FSC) and side scatter (SSC). Created with  
133 BioRender.

### 134 2.3 Data cleaning

135 Although the samples were filtered to retain only particles within the size range of pollen grains ( $5\text{-}100\mu\text{m}$ ),  
136 some non-pollen particles, such as dust or plant debris, were still present. To distinguish pollen from debris,  
137 that is non-pollen particles, we used the recorded size, granularity, and fluorescence parameters for each  
138 particle. These include one value for size (FSC), one for granularity (SSC), and ten values for fluorescence,  
139 each with two components, the maximum peak height and the peak area except size which has also a width  
140 component. This resulted in three values for size, two for granularity, and 20 for fluorescence, with a total  
141 of 25 parameter values per particle.

142 Data cleaning was performed using Cytexpert software version 2.4.28 (Beckman Coulter, Inc.). For each  
143 species, pollen grains were manually separated from debris using scatter density plots (size vs. granularity)

144 and histograms of all fluorescence features. This selection relied primarily on the PB450 ( $\lambda=450/45\text{nm}$ ) and  
145 Violet610 ( $\lambda=610/20\text{nm}$ ) fluorescence histograms, while cross-checking against the other recorded  
146 parameters to ensure consistency. Adjustments were made as needed to ensure that only true pollen grains  
147 were retained (Fig. A2). This excitation/emission range is characteristic of sporopollenin which contains  
148 the fluorophores specific to pollen grains (Pöhlker et al., 2013). The final training dataset included all  
149 cleaned pollen data from each species along with a separate category, “OTHER”, which combined all debris  
150 data from the cleaning step and the particles from certain species for which it was impossible to distinguish  
151 pollen from debris, such as those in the *Thuja* genus. The final reference database used to train the model  
152 comprised 97 species from 34 different genera. A detailed list of species is presented in Table A1 and the  
153 complete training datasets are available on Figshare (Tardif, 2025).

## 154 2.4 Machine learning algorithm

155 Four supervised classification algorithms were initially tested: *Random Forest* (Breiman, 2021), *Gradient*  
156 *Boosting*, *Extreme Gradient Boosting* and *Neuronal Network*. Among these, the Random Forest algorithm  
157 showed the best performance using F1-scores and was therefore selected for subsequent analysis. In our  
158 training dataset, the number of pollen grains varies across taxa (Table A2). This caused the model to more  
159 frequently predict taxa with more training examples (Chawla, 2010). To address this class imbalance, we  
160 used the synthetic minority over-sampling technique (Chawla, 2010), resulting in a balanced dataset with  
161 1,000 pollen grains per species for the species-level classification model and 10,000 pollen grains per genus  
162 for the genus-level classification model. Only four taxa were oversampled (*Acer saccharum*, *Gramineae*  
163 *spp*, *Juglans cinerea*, and *Picea abies*). The purpose of balancing data was to provide the classifier with a  
164 balanced training set to prevent it from being biased toward the majority class. Each dataset was randomly  
165 split into two subsets: 70% for training and 30% for validation. The validation set, was not used for model  
166 training. The Random Forest classifier was trained exclusively on the 70% training portion. Models were  
167 trained using the *train()* function from the *caret* package in R software (version 4.4.0), calling the *rf()*  
168 function for the random forest model. Model robustness was assessed using 10-fold cross-validation  
169 implemented via the *trainControl()* function with the “cv” method (nine repetitions for training and one for  
170 validation). We trained the models using the default value of 500 trees. The parameter *mtry*, representing  
171 the number of variables randomly selected at each node split, was set to 5, based on prior testing across  
172 values from 1 to 10. We assessed the models’ performance using the  $F_1$ -score:  $F_1 =$   
173  $(2 * \text{precision} * \text{recall}) / (\text{precision} + \text{recall})$ . Precision is the proportion of correctly predicted positives out of  
174 all predicted positives and recall is the proportion of correctly predicted positives out of all actual positives  
175 (Grandini et al., 2020). Variable importance was assessed using the mean decrease in Gini coefficient,

176 which quantifies each variable's contribution to reducing classification error by decreasing node impurity  
177 during tree construction. The trained models are available on Figshare (Tardif, 2025).

## 178 **3 Results**

### 179 **3.1 Classification performance**

180 At the species level, the model achieved a mean  $F_1$ -score of 0.76 (n=97 species; Fig. 2a). Most species  
181 perform very well, with 75% of species achieving a  $F_1$ -score above 0.70. The lowest  $F_1$ -scores were  
182 obtained for *Quercus rubra* (0.44), *Salix x pendulina f. tristis*. (*Salix alba tristis* hereafter) (0.43) and *Ulmus*  
183 *minor* (0.44). Several other species also showed reduced accuracy, with  $F_1$ -scores ranging between 0.5 and  
184 0.65. These included *Acer x freemanii*, *Acer ukurunduense*, *Fagus grandifolia*, *Fraxinus nigra*, *Pinus*  
185 *banksiana*, and *Syringa villosa*, as well as several species of the Betulaceae family (*Betula papyrifera*,  
186 *Carpinus caroliniana*, and *Corylus colurna*), the Juglandaceae family (*Carya ovata*, *Juglans nigra*, and  
187 *Juglans virginiana*), and the *Ulmus* genus (*Ulmus davidiana*, *Ulmus propinqua*, and *Ulmus pumila*) (Fig.  
188 2a).

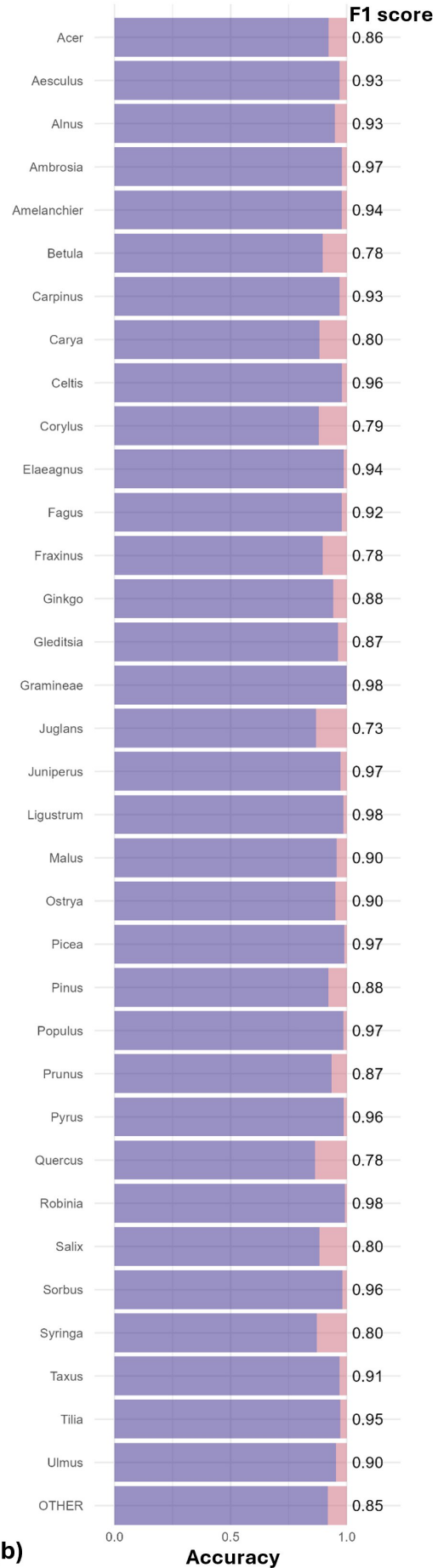
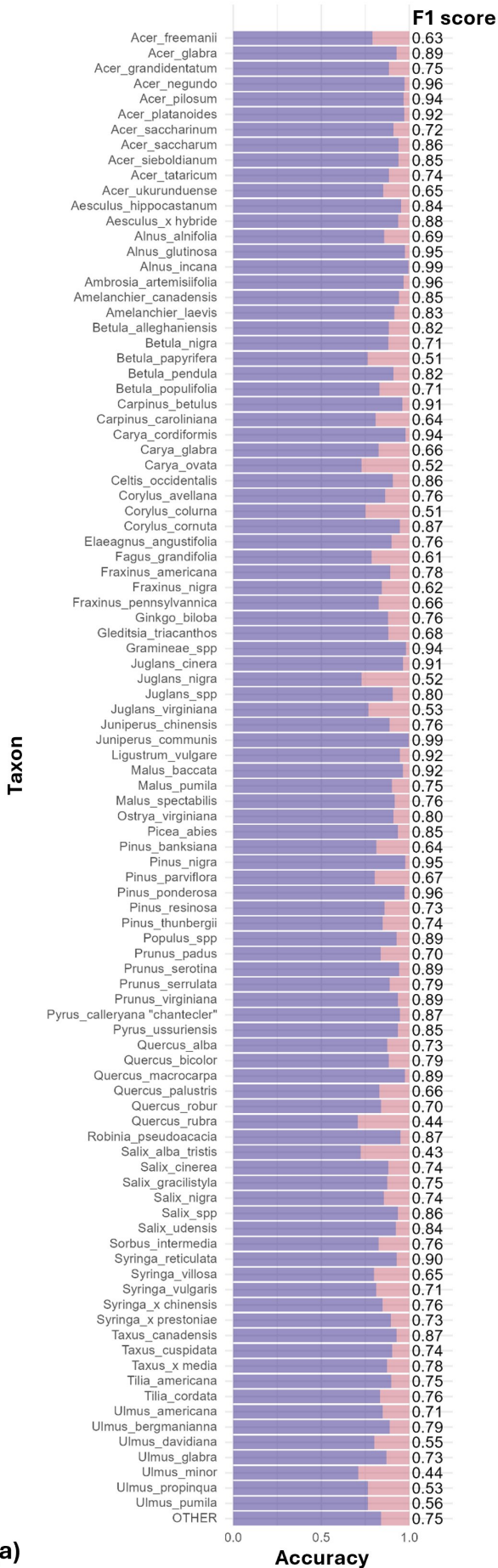
189 When trained at the genus level, model performance improved across the 34 genera, reaching a mean  $F_1$ -  
190 score of 0.90 (Fig. 2b). The only notable exception was *Juglans*, with an  $F_1$ -score of 0.73. All other genera  
191 achieved  $F_1$ -scores close to or above 0.8. Taxa with relatively lower accuracy at the species level, such as  
192 those in the genera *Betula*, *Quercus* and *Ulmus*, showed marked improvement at the genus level. Most  
193 misclassifications occurred between species within the same genus, as is evident for species from the genus  
194 *Ulmus* (see confusion matrices in Appendix B and in supplement material Table S1 and Table S2).

### 195 **3.2 Variables contribution**

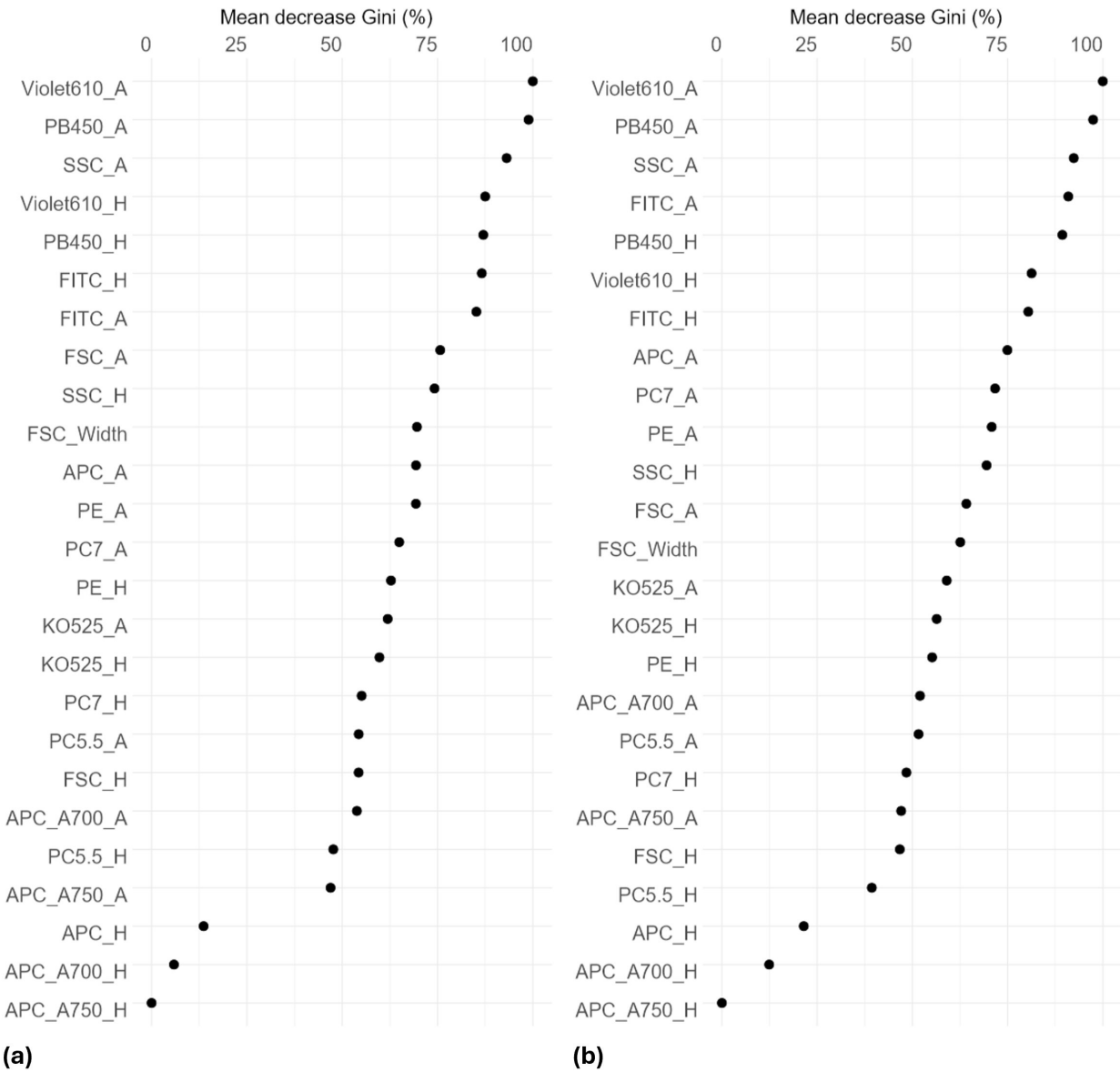
196 The ranking of predictors using the Gini index shows that the most important variables for distinguishing  
197 pollen grains among taxa were granularity (SSC), two fluorescence variables from the violet laser (PB450  
198 and Violet610) and one from the blue laser (FITC). These variables exhibited the highest mean decrease in  
199 Gini, indicating a major contribution to the homogeneity of nodes and consequently, to overall classification  
200 accuracy in the Random Forest model (Fig. 3).

201 Analysis of the variables contributing most to pollen differentiation revealed that size (FSC) and granularity  
202 (SSC) varied more among genera than among species within a given genus, whereas fluorescence  
203 parameters primarily accounted for the variation observed among species within genera (Fig.4 and  
204 Appendix C). Figure 4 illustrates the distributions for six genera known to be allergenic (see Appendix C  
205 for more details). Pollen grains from the *Pinus* genus were larger than those from other genera and also had

206 a specific granularity pattern. For these two parameters, FSC and SSC, intra-genus variation for all genera  
207 was very small or absent. In contrast, fluorescence parameters showed more pronounced differences among  
208 species within the same genus. For example, *Alnus* species presented distinct values across all three  
209 fluorescence channels (FITC, Violet610, PB450), while *Corylus* species differed mainly in the Violet610  
210 channel. For other genera, only certain species, such as *Betula nigra*, *Quercus macrocarpa*, and *Salix spp.*,  
211 showed distinct fluorescence profiles (Fig. 4).

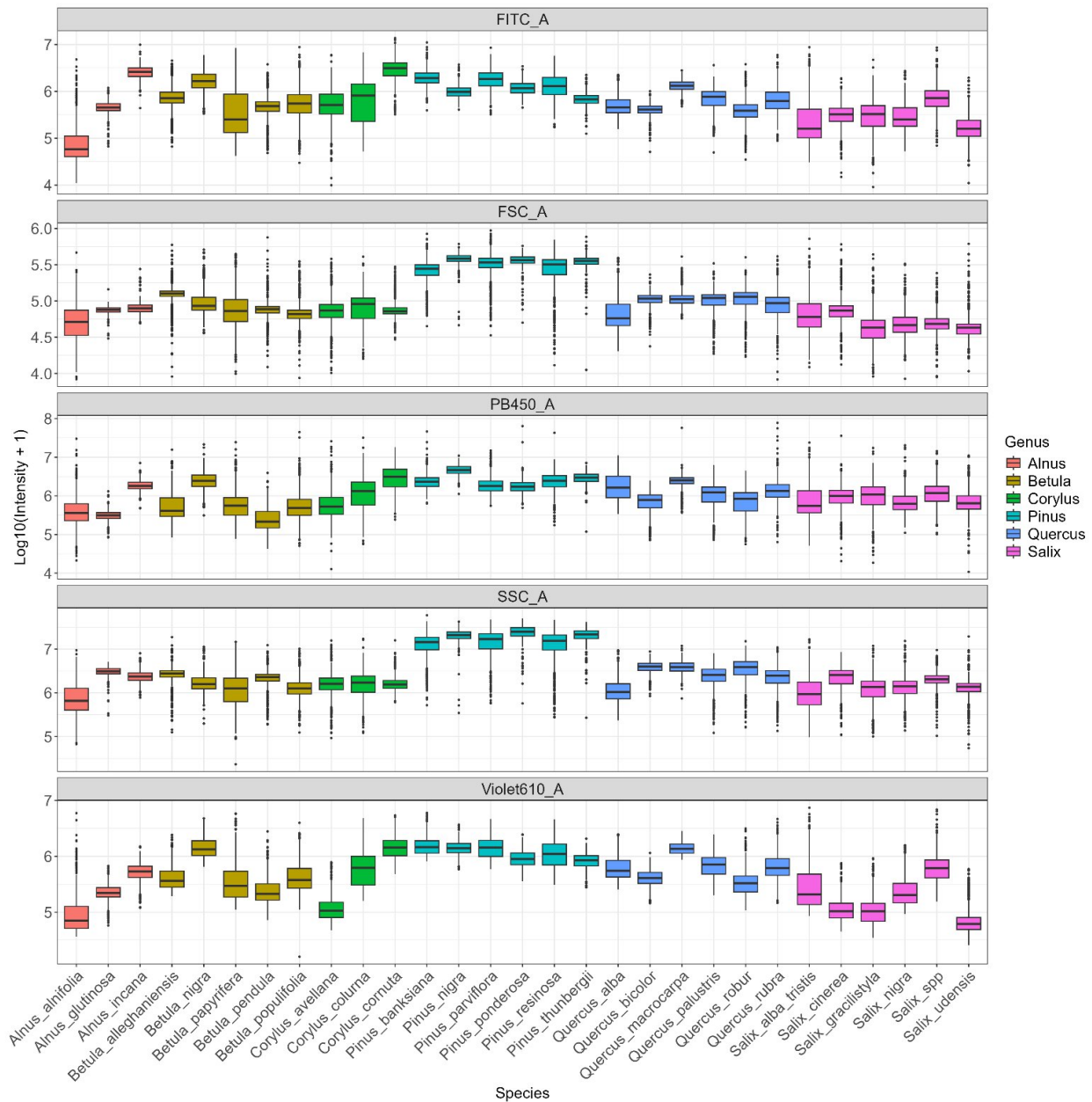


213 **Figure 2:** Performance of the classification models at the species (a) and genus levels (b). For each taxon,  
 214 purple bars represent correct classifications (accuracy) and pink represents misclassifications (1-accuracy).  
 215 F<sub>1</sub>-scores are shown as labels to the right of each bar. Mean F<sub>1</sub>-scores were 0.76 for the species-level model  
 216 and 0.90 for the genus-level model.



217 **(a)** **(b)**

218 **Figure 3:** Variable contributions to node and leaf purity in the Random Forest classification model,  
 219 measured by mean decrease in Gini index. Higher values indicate greater importance. Results are shown  
 220 for species-level (a) and genus-level (b) models. Each variable includes two metrics: maximum peak height  
 221 (H) and peak area (A). Explanation of variable names in FigureA1.



223

224 **Figure 4:** Distribution of log-transformed values for the five variables that contributed the most to  
 225 distinguish species. Fluorescence channels: FITC\_A (excitation: 488 nm/emission: 525 nm), PB450\_A  
 226 (excitation: 405 nm/ emission: 450 nm), Violet610\_A (excitation: 405 nm/ emission: 610 nm); scatter  
 227 parameters: SSC\_A (granularity) and FSC\_A (size). The suffix \_A indicates that we consider the signal's  
 228 peak area. Only species from six known allergenic genera (*Alnus*, *Betula*, *Corylus*, *Pinus*, *Quercus*, *Salix*)  
 229 are shown and coloured. For all species see Appendix C.

230

## 231 4 Discussion

232 Our results demonstrate that flow cytometry combined with machine learning can reliably identify pollen  
233 across a wide range of taxa. The models achieved high classification performance ( $F_1=0.76$  at the species  
234 level and 0.90 at the genus level) highlighting the potential of this approach as a scalable alternative to  
235 traditional microscopy for pollen identification. This represents a significant improvement over  
236 conventional methods, such as microscopy, which typically only resolve pollen to the genus or family level.  
237 The improved performance of the genus-level model over the species-level model most likely reflects  
238 biological and structural similarities among species within the same genus. This was particularly evident  
239 for species in the *Betulaceae* family, which are wind-pollinated and considered highly allergenic (D'Amato  
240 et al., 2007; Falagiani, 1989), but also for other genera especially abundant in Montreal, such as *Acer*,  
241 *Syringa*, and *Ulmus*. While these findings are promising, they were obtained using reference pollen grains  
242 collected directly on trees; further validation using atmospheric samples will be necessary before  
243 implementation in an airborne pollen monitoring network.

244 The advantage of flow cytometry coupled with machine learning lies not only in its performance in  
245 classifying at the genus or species level, but especially in its ability to enable automated, high-throughput  
246 identification ( $\approx 5000$  grains $\cdot$ s $^{-1}$ ) while avoiding the lengthy and costly training required for human  
247 specialists. Accurate monitoring is clinically important, as even low pollen concentrations (10–50 grains  
248 per cubic meter) can trigger allergic symptoms (Steckling-Muschack et al., 2021). From a public health  
249 perspective, the genus-level model is therefore appropriate, as it provides higher accuracy for the taxa most  
250 relevant to allergy monitoring.

251 The fluorescence variables that contributed most to pollen classification were associated with blue and  
252 violet excitation lasers, with emission detected in the blue (PB450), red-orange (Violet610), and green  
253 (FITC) channels. This pattern is consistent with the known autofluorescence properties of sporopollenin,  
254 the main biopolymer in the pollen exine, which emits strongly near 475 nm (Pöhlker et al., 2013). Additional  
255 emissions likely originate from secondary compounds such as flavonoids, carotenoids, and terpenes located  
256 in the exine or pollenkitt coating (Donaldson, 2020; Pöhlker et al., 2013). The distribution of the most  
257 discriminative variables indicates that size and granularity primarily differentiate genera, while blue, red-  
258 orange and green fluorescence channels capture species-level differences within genera. This pattern  
259 explains the model's higher accuracy at the genus-level and its partial success in distinguishing closely  
260 related species. The misclassifications at species-level likely stem from the high similarity in pollen shape  
261 and fluorescence spectra among closely related species, which makes them harder to distinguish. In addition,  
262 because our classification relied on size and fluorescence alone, without complementary morphological

263 data such as holography images (Erb et al., 2024; Gierlicka et al., 2022; Zhang and Abdulla, 2023), the  
264 model's performance may have been constrained by limited representation of some taxa in the reference  
265 dataset. Increasing both the number of pollen grains per species and the diversity of species within each  
266 genus would help train more robust models. Future research should prioritize expanding reference datasets,  
267 ideally through the creation of a global database of pollen fluorescence signatures, which represent the  
268 emission spectrum for given excitation wavelengths. Such a resource, similar to *The Global Pollen Project*,  
269 for microscopic images (Martin and Harvey, 2017), would provide a valuable foundation for machine  
270 learning and deep learning applications in aerobiology, but also ecology, palynology, paleoecology, and  
271 other pollen related fields.

272 Another factor that may explain the reduced model accuracy is that some species in our reference collection  
273 could not be included in the model's training dataset due to the impossibility to distinguish pollen from  
274 debris during the data cleaning, even though we had visually confirmed the presence of intact pollen grains  
275 in our samples. These data were included in the training dataset under the category "OTHER" rather than  
276 assigned to individual taxa. Such was the case for *Thuja*, a genus abundant in Montreal (Paquette et al.,  
277 2026), likely due to the small size of its pollen grains, which can easily mix with debris or because pollen  
278 grains included in our dataset may have been limited in quantity or had not fully matured. Indeed,  
279 distinguishing male from female *Thuja* cones and assessing the phenological stage to collect mature pollen  
280 is difficult, and the small size of the cones is another challenge for pollen extraction. Improving collection  
281 and extraction protocols for this genus could help reduce debris contamination in future sampling.

282 A crucial next step is to adapt these models for use on complex airborne samples collected in urban  
283 environments. Such samples often contain large amounts of debris as during atmospheric transport, pollen  
284 grains may remain airborne for days or weeks, during which they can fold, crack, or adhere to air pollutants  
285 (De Weger et al., 2024). They are also exposed to ultraviolet radiation and humidity fluctuations that can  
286 alter fluorescence properties. These factors complicate the discrimination of true pollen grains from other  
287 particles and represent a major challenge for operational implementation.

288 Because small pollen grains, folded grains and debris can have overlapping size distributions,  
289 misclassification remains a possibility, with pollen occasionally identified as debris, and vice versa. Future  
290 research could therefore explore multidimensional hierarchical classification frameworks, especially when  
291 complementarity data such as holographic images are available for validation. For example, when  
292 classification confidence is high, the model could assign a species-level label, but default to a broader  
293 taxonomic category such as genus or family when uncertainty is greater (Hernández et al., 2014). This

294 flexibility would prevent incorrect fine-level classifications and improve overall reliability under complex  
295 environmental conditions.

296 Another limitation of flow cytometry-based models concerns their device dependency, as fluorescence  
297 intensity values are typically linked to the specific cytometer used during model training, which limits  
298 model transferability across instruments and comparison to other measurement. However, deployment  
299 within harmonized analyzers is feasible under standard bead-based daily QC protocols (CS&T/Application  
300 Settings for conventional analyzers; SpectroFlo QC beads for spectral systems), which have been shown to  
301 control inter-instrument MFI drift within single-digit percentages (Cornel et al., 2020; Omana-Zapata et al.,  
302 2019; Solly et al., 2013b). Channel-wise normalization during data processing further reduces residual  
303 variability, and a lightweight domain-adaptation step, based on acquiring a small reference pollen set on the  
304 target instrument, can re-anchor feature distributions prior to inference. FSC and SSC parameters remain  
305 more sensitive to flow-rate and optical alignment and should therefore be monitored carefully. Where direct  
306 comparison between instruments is required, ERF/MESF calibration from NIST's Flow Cytometry  
307 Standards Consortium allows comparing fluorescence results between different instruments (Wang and  
308 Hoffman, 2017). Standardization procedures, such as calibrating cytometers using Rainbow beads and  
309 Quality Control beads could help ensure consistent signal outputs across different instruments (Solly et al.,  
310 2013). The present work was carried out using a conventional cytometer with three lasers and ten filters;  
311 using equipment with more lasers and detectors could refine the detection of fluorescent signatures and  
312 detect more of them. Spectral cytometry also opens up new possibilities for analyzing fluorescent signatures  
313 on a larger scale (Konecny et al., 2024), which could enable even better characterization of pollen based on  
314 its fluorescence.

315 The combination of flow cytometry and a Random Forest classification model proves to be a highly  
316 promising approach for the identification of airborne pollen in urban environments. By relying exclusively  
317 on routinely measured cytometric parameters, rather than images, this method ensures broad applicability  
318 and compatibility with standard healthcare and clinical cytometers. Integrating this approach into existing  
319 aerobiological monitoring networks could enable faster identification and quantification of allergenic  
320 pollen. We also built an extensive reference pollen collection comprising 97 species across 34 genera. For  
321 each species, we have several floral units (flower, catkins, cones) containing pollen, microscopic slides, and  
322 flow cytometry data for all pollen grains. This reference collection could be reused for different purposes  
323 such as future model training.

## 324 **5 Conclusion**

325 This study demonstrates a significant advancement in pollen identification by combining flow cytometry  
326 with a Random Forest classification model. This approach achieved high accuracy at both the genus ( $F_1 =$   
327 0.90) and species levels ( $F_1 = 0.76$ ), surpassing several limitations of traditional microscopy. While species-  
328 level classification remains challenging for certain taxa, the results highlight the method's robustness and  
329 potential for large-scale implementation. With continued refinement and standardization, this approach  
330 could enable faster cheap, high throughput pollen identification and broaden its applications in  
331 aerobiological monitoring, while supporting public health applications and advancing research in pollen  
332 ecology worldwide.

### 333 **6 Code availability**

334 The code is available on the public Github repository SarahTardif/Pollen-classification-model.

### 335 **7 Data availability**

336 Training datasets and trained models are available on a Figshare repository  
337 (<https://doi.org/10.6084/m9.figshare.30870641>). More data can be provided upon request.

### 338 **8 Author contribution**

339 ST: conceptualization, data collection, analyses, writing – original draft; AP, ILL, and RSS:  
340 conceptualization, funding acquisition, supervision, validation, support, writing – review and editing; GB:  
341 methodology (cytometry), writing – review and editing; MRK: methodology (lab protocols), writing –  
342 review and editing; GL: methodology (initial algorithm for the machine learning model), writing – review  
343 and editing

### 344 **9 Competing interests**

345 The authors declare that they have no conflict of interest.

### 346 **10 Acknowledgements**

347 We thank the CERMO-UQAM Imaging Platform and the Aerobiology Research Laboratories for their  
348 technical support. We are grateful for the precious help of Kira Safranova, Emily Ducharme, Maya Héon,  
349 and Kim Florentin in sampling, filtering, and running fresh pollen through the cytometer. We thank the  
350 Montreal Botanical Garden for permitting pollen collection from tree flowers. Model training was  
351 performed on supercomputers managed by Calcul Québec and the Digital Research Alliance of Canada.

352 **11 Financial support**

353 This work was funded by NSERC-Alliance ALLRP 554373 – 21 and *Fonds vert dans le cadre du Plan*

354 *d'action 2013-2020 sur les changements climatiques du gouvernement québécois* awarded to AP.

355 ST also received funding from the Urban forestry program NSERC-CREATE -543300-20.

356 **Appendix A: Reference pollen collection**357 **Table A1:** Species in the reference pollen collection

Family	Genus	Species (scientific name)	Authority
Asteraceae	<i>Ambrosia</i>	<i>Ambrosia artemisiifolia</i>	L.
Betulaceae	<i>Alnus</i>	<i>Alnus alnifolia</i>	Mill.
		<i>Alnus glutinosa</i>	(L.) Gaertn.
		<i>Alnus incana</i>	(L.) Moench
	<i>Betula</i>	<i>Betula alleghaniensis</i>	Britton
		<i>Betula nigra</i>	L.
		<i>Betula papyrifera</i>	Marshall
		<i>Betula pendula</i>	Roth
	<i>Carpinus</i>	<i>Betula populifolia</i>	Marshall
		<i>Carpinus betulus</i>	L.
		<i>Carpinus caroliniana</i>	Walter
	<i>Corylus</i>	<i>Corylus avellana</i>	L.
		<i>Corylus colurna</i>	L.
<i>Corylus cornuta</i>		Marshall	
<i>Ostrya</i>	<i>Ostrya virginiana</i>	(Mill.) K.Koch	
Cannabacées	<i>Celtis</i>	<i>Celtis occidentalis</i>	L.
Cupressaceae	<i>Juniperus</i>	<i>Juniperus chinensis</i>	L.
		<i>Juniperus communis</i>	L.
Elaeagnaceae	<i>Elaeagnus</i>	<i>Elaeagnus angustifolia</i>	L.
Fabaceae	<i>Gleditsia</i>	<i>Gleditsia triacanthos</i>	L.
	<i>Robinia</i>	<i>Robinia pseudoacacia</i>	L.
Fagaceae	<i>Fagus</i>	<i>Fagus grandifolia</i>	Ehrh.
	<i>Quercus</i>	<i>Quercus alba</i>	L.
		<i>Quercus bicolor</i>	Willd.
		<i>Quercus macrocarpa</i>	Michx.
		<i>Quercus palustris</i>	Mnchh.
		<i>Quercus robur</i>	L.
<i>Quercus rubra</i>	L.		
Ginkgoaceae	<i>Ginkgo</i>	<i>Ginkgo biloba</i>	L.
Gramineae/Poaceae	-	<i>Gramineae spp</i>	
Juglandaceae	<i>Carya</i>	<i>Carya cordiformis</i>	(Wangenh.) K.Koch
		<i>Carya glabra</i>	(Mill.) Sweet
		<i>Carya ovata</i>	(Mill.) K.Koch
	<i>Juglans</i>	<i>Juglans cinerea</i>	L.
		<i>Juglans nigra</i>	L.
		<i>Juglans spp</i>	L.
		<i>Juglans virginiana</i>	L.

Family	Genus	Species (scientific name)	Authority
Oleaceae	<i>Fraxinus</i>	<i>Fraxinus americana</i>	L.
		<i>Fraxinus nigra</i>	Marshall
		<i>Fraxinus pennsylvannica</i>	Marshall
	<i>Ligustrum</i>	<i>Ligustrum vulgare</i>	L.
	<i>Syringa</i>	<i>Syringa reticulata</i>	(Blume) H.Hara
		<i>Syringa villosa</i>	Vahl
		<i>Syringa vulgaris</i>	L.
		<i>Syringa x chinensis</i>	Willd.
<i>Syringa x prestoniae</i>		McKelvey	
Pinaceae	<i>Picea</i>	<i>Picea abies</i>	(L.) H.Karst.
	<i>Pinus</i>	<i>Pinus banksiana</i>	Lamb.
		<i>Pinus nigra</i>	J.F.Arnold
		<i>Pinus parviflora</i>	Siebold & Zucc.
		<i>Pinus ponderosa</i>	Douglas ex C.Lawson
		<i>Pinus resinosa</i>	Aiton
		<i>Pinus thunbergii</i>	Parl.
Rosaceae	<i>Amelanchier</i>	<i>Amelanchier canadensis</i>	(L.) Medik.
		<i>Amelanchier laevis</i>	Wiegand
	<i>Malus</i>	<i>Malus baccata</i>	(L.) Borkh.
		<i>Malus pumila</i>	Mill.
		<i>Malus spectabilis</i>	(Aiton) Borkh.
	<i>Prunus</i>	<i>Prunus padus</i>	L.
		<i>Prunus serotina</i>	Ehrh.
		<i>Prunus serrulata</i>	Lindl.
		<i>Prunus virginiana</i>	L.
	<i>Pyrus</i>	<i>Pyrus calleryana "chantecler"</i>	Decne.
		<i>Pyrus ussuriensis</i>	Maxim.
<i>Sorbus</i>	<i>Sorbus intermedia</i>	Ehrh.	
Salicaceae	<i>Populus</i>	<i>Populus spp</i>	L.
	<i>Salix</i>	<i>Salix alba tristis</i>	Gaudin
		<i>Salix cinerea</i>	L.
		<i>Salix gracilistyla</i>	Miq.
		<i>Salix nigra</i>	Marshall
		<i>Salix spp</i>	
		<i>Salix udensis</i>	(Wimm.) Trautv. & C.A.Mey.

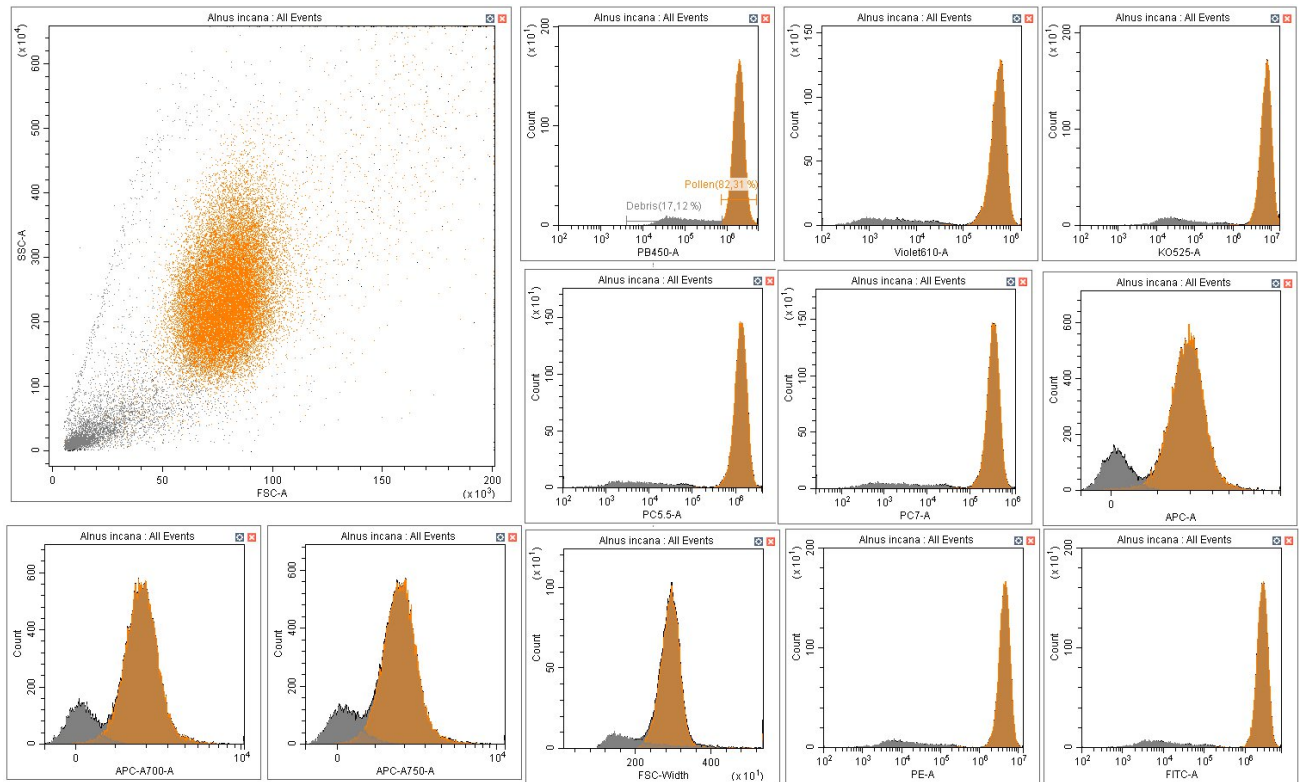
Family	Genus	Species (scientific name)	Authority
Sapindaceae	Acer	<i>Acer freemanii</i>	A.E.Murray
		<i>Acer glabra</i>	Torr.
		<i>Acer grandidentatum</i>	Nutt. ex Torr. & A.Gray
		<i>Acer negundo</i>	L.
		<i>Acer pilosum</i>	Maxim.
		<i>Acer platanoides</i>	L.
		<i>Acer saccharinum</i>	L.
		<i>Acer saccharum</i>	Marshall
		<i>Acer sieboldianum</i>	Miq.
		<i>Acer tataricum</i>	L.
	<i>Acer ukurunduense</i>	Trautv. & C.A.Mey.	
	Aesculus	<i>Aesculus hippocastanum</i>	L.
<i>Aesculus x hybride</i>		DC.	
Taxaceae	Taxus	<i>Taxus canadensis</i>	Marshall
		<i>Taxus cuspidata</i>	Siebold & Zucc.
		<i>Taxus x media</i>	Rehder
Tiliaceae	Tilia	<i>Tilia americana</i>	L.
		<i>Tilia cordata</i>	Mill.
Ulmaceae	Ulmus	<i>Ulmus americana</i>	L.
		<i>Ulmus bergmanianna</i>	C.K.Schneid.
		<i>Ulmus davidiana</i>	Planch.
		<i>Ulmus glabra</i>	Huds.
		<i>Ulmus minor</i>	Mill.
		<i>Ulmus propinqua</i>	Koidz.
<i>Ulmus pumila</i>	L.		

Detector name	PB 450	KO 525	Violet 610	PE	FITC	PC5,5	PC7	APC	APC- A700	APC- A750	Granularity	Size
											SSC	FSC
Excitation (nm)	405			488				640			-	-
Emission (nm)	450	525	610	585	525	690	780	660	712	780	-	-

360

361 **Figure A1:** Explanation of cytometry variable names, showing the respective excitation lasers and emission

362 detectors with their wavelengths and associated colors.



363

364 **Figure A2:** Distinction pollen (orange) versus debris (grey) on CytExpert software: Example of *Alnus*  
 365 *incana*

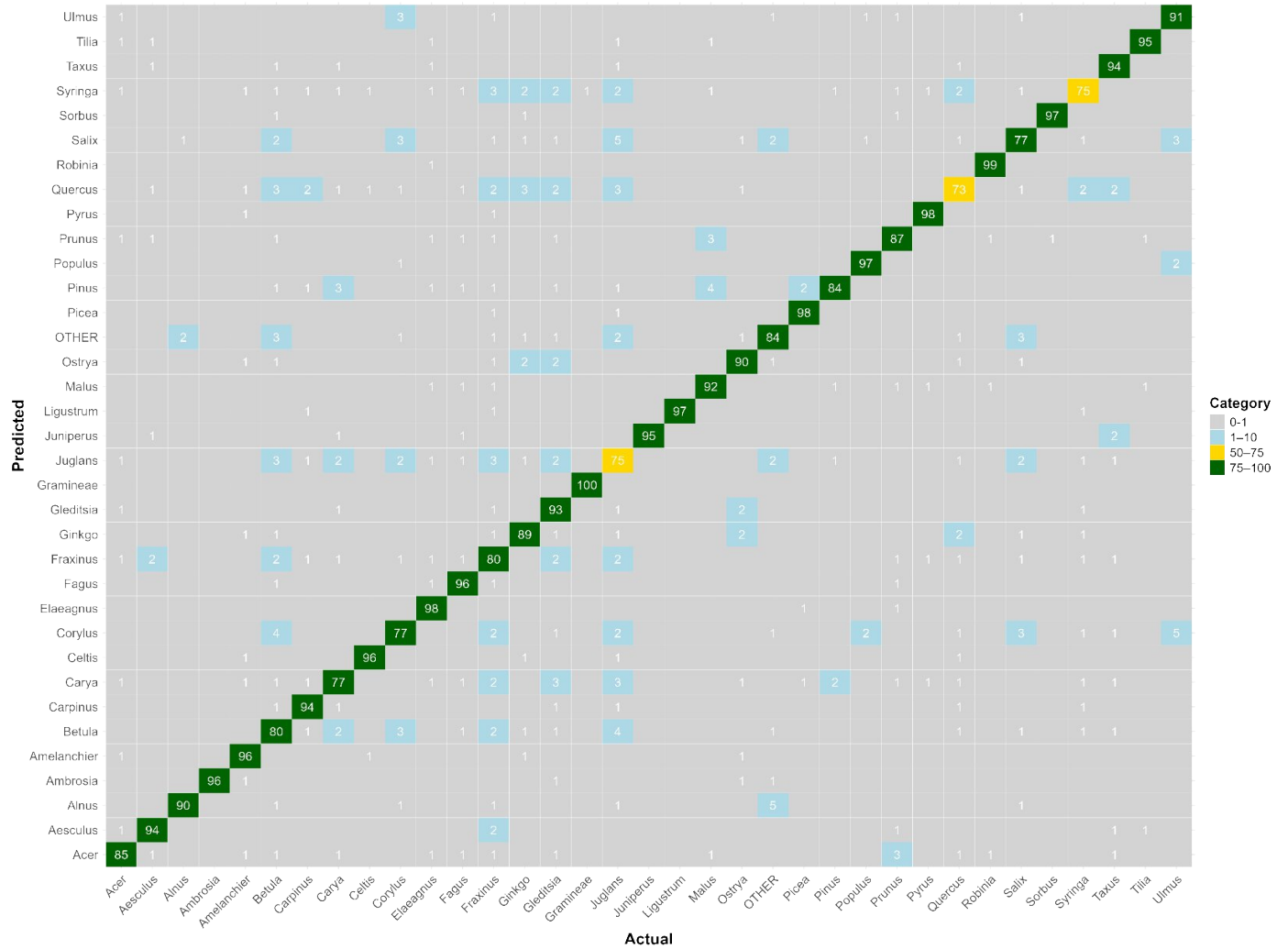
366 **Table A2:** Number of pollen grains per species in the training dataset before balancing data

Species	Freq_pollen
<i>Acer_freemanii</i>	2095
<i>Acer_glabra</i>	8259
<i>Acer_grandidentatum</i>	4324
<i>Acer_negundo</i>	15603
<i>Acer_pilosum</i>	9220
<i>Acer_platanoides</i>	2726
<i>Acer_saccharinum</i>	3674
<i>Acer_saccharum</i>	447
<i>Acer_sieboldianum</i>	11089
<i>Acer_tataricum</i>	2605
<i>Acer_ukurunduense</i>	3860
<i>Aesculus_hippocastanum</i>	8278
<i>Aesculus_x hybride</i>	11041
<i>Alnus_alnifolia</i>	10517
<i>Alnus_glutinosa</i>	21586
<i>Alnus_incana</i>	28158

<i>Ambrosia artemisiifolia</i>	33615
<i>Amelanchier canadensis</i>	1552
<i>Amelanchier laevis</i>	3836
<i>Betula alleghaniensis</i>	5780
<i>Betula nigra</i>	4954
<i>Betula papyrifera</i>	13163
<i>Betula pendula</i>	2151
<i>Betula populifolia</i>	21222
<i>Carpinus betulus</i>	2973
<i>Carpinus caroliniana</i>	1580
<i>Carya cordiformis</i>	9603
<i>Carya glabra</i>	3256
<i>Carya ovata</i>	7579
<i>Celtis occidentalis</i>	3238
<i>Corylus avellana</i>	10290
<i>Corylus colurna</i>	4404
<i>Corylus cornuta</i>	1232
<i>Elaeagnus angustifolia</i>	2998
<i>Fagus grandifolia</i>	1428
<i>Fraxinus americana</i>	3689
<i>Fraxinus nigra</i>	2759
<i>Fraxinus pennsylvannica</i>	8732
<i>Ginkgo biloba</i>	12685
<i>Gleditsia triacanthos</i>	7674
<i>Gramineae spp</i>	988
<i>Juglans cinerea</i>	306
<i>Juglans nigra</i>	9867
<i>Juglans spp</i>	11972
<i>Juglans virginiana</i>	2886
<i>Juniperus chinensis</i>	5544
<i>Juniperus communis</i>	35307
<i>Ligustrum vulgare</i>	4278
<i>Malus baccata</i>	2328
<i>Malus pumila</i>	3141
<i>Malus spectabilis</i>	6241
<i>Ostrya virginiana</i>	26203
<i>Picea abies</i>	881
<i>Pinus banksiana</i>	2722
<i>Pinus nigra</i>	14008
<i>Pinus parviflora</i>	2897
<i>Pinus ponderosa</i>	1991
<i>Pinus resinosa</i>	7670
<i>Pinus thunbergii</i>	2751
<i>Populus spp</i>	4720

<i>Prunus_padus</i>	1407
<i>Prunus_serotina</i>	1878
<i>Prunus_serrulata</i>	5575
<i>Prunus_virginiana</i>	1242
<i>Pyrus_calleryana</i> "chantecler"	1685
<i>Pyrus_ussuriensis</i>	1042
<i>Quercus_alba</i>	11635
<i>Quercus_bicolor</i>	17603
<i>Quercus_macrocarpa</i>	13868
<i>Quercus_palustris</i>	8956
<i>Quercus_robur</i>	23812
<i>Quercus_rubra</i>	6899
<i>Robinia_pseudoacacia</i>	1828
<i>Salix_alba_tristis</i>	7484
<i>Salix_cinerea</i>	7372
<i>Salix_gracilistyla</i>	6600
<i>Salix_nigra</i>	11276
<i>Salix_spp</i>	7741
<i>Salix_udensis</i>	18766
<i>Sorbus_intermedia</i>	1472
<i>Syringa_reticulata</i>	2351
<i>Syringa_villosa</i>	10681
<i>Syringa_vulgaris</i>	8695
<i>Syringa_x_chinensis</i>	11478
<i>Syringa_x_prestoniae</i>	11520
<i>Taxus_canadensis</i>	4181
<i>Taxus_cuspidata</i>	19143
<i>Taxus_x_media</i>	17655
<i>Tilia_americana</i>	3428
<i>Tilia_cordata</i>	8802
<i>Ulmus_americana</i>	3622
<i>Ulmus_bergmanianna</i>	1337
<i>Ulmus_davidiana</i>	1050
<i>Ulmus_glabra</i>	1340
<i>Ulmus_minor</i>	1905
<i>Ulmus_propinqua</i>	5762
<i>Ulmus_pumila</i>	8377
OTHER	100000



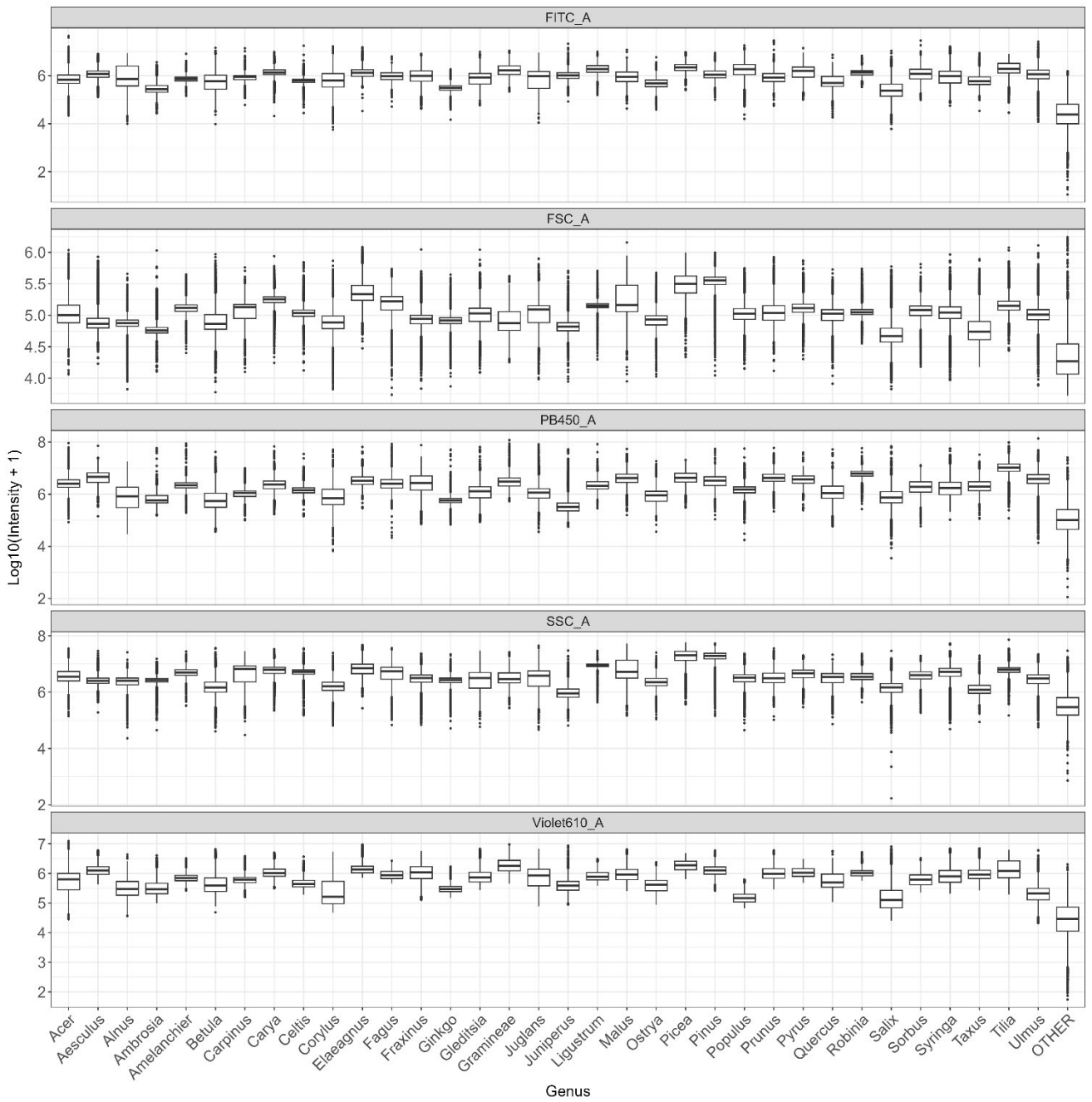


375

376 **Figure B2:** Confusion matrix for the genus-level model. The values represent, for each genus, the  
 377 percentage of pollen grains correctly classified (on the diagonal) and misclassified with the actual  
 378 corresponding genus (on the x-axis). Colors correspond to categories (0–1% in gray, 1–10% in blue,  
 379 10–50% in red, 50–75% in yellow, and 75–100% in green). Raw data are provided in supplemental  
 380 Table S2.

381 **Appendix C: Distributions of values for the main discriminant variables.**

382



383

384 **Figure C1:** Distribution of log-transformed values for the variables that contribute the most to distinguish  
 385 taxa (FITC,FSC,SSC,Violet610, PB450) across all genera.



389 **References**

- 390 Ahlholm, Helander, and Savolainen: Genetic and environmental factors affecting the allergenicity of birch  
391 (*Betula pubescens* ssp. *czerepanovii* [Orl.] Hämet-Ahti) pollen, *Clinical & Experimental Allergy*, 28,  
392 1384–1388, <https://doi.org/10.1046/j.1365-2222.1998.00404.x>, 1998.
- 393 Aloisi, I., Cai, G., Tumiatti, V., Minarini, A., and Del Duca, S.: Natural polyamines and synthetic analogs  
394 modify the growth and the morphology of *Pyrus communis* pollen tubes affecting ROS levels and causing  
395 cell death, *Plant Science*, 239, 92–105, <https://doi.org/10.1016/j.plantsci.2015.07.008>, 2015.
- 396 Anderegg, W. R. L., Abatzoglou, J. T., Anderegg, L. D. L., Bielory, L., Kinney, P. L., and Ziska, L.:  
397 Anthropogenic climate change is worsening North American pollen seasons, *Proc. Natl. Acad. Sci. U.S.A.*,  
398 118, e2013284118, <https://doi.org/10.1073/pnas.2013284118>, 2021.
- 399 Breiman, L.: *Random forests*. Machine learning, 2001.
- 400 Brennan, G. L., Potter, C., de Vere, N., Griffith, G. W., Skjøth, C. A., Osborne, N. J., Wheeler, B. W.,  
401 McInnes, R. N., Clewlow, Y., Barber, A., Hanlon, H. M., Hegarty, M., Jones, L., Kurganskiy, A., Rowney,  
402 F. M., Armitage, C., Adams-Groom, B., Ford, C. R., Petch, G. M., and Creer, S.: Temperate airborne grass  
403 pollen defined by spatio-temporal shifts in community composition, *Nat Ecol Evol*, 3, 750–754,  
404 <https://doi.org/10.1038/s41559-019-0849-7>, 2019.
- 405 Chawla, N. V.: Data mining for imbalanced datasets: An overview, in: *Data mining and knowledge*  
406 *discovery handbook*, 875–886, 2010.
- 407 Cornel, A. M., Van Der Burght, C. A. J., Nierkens, S., and Van Velzen, J. F.: FACSCanto II and  
408 LSRFortessa flow cytometer instruments can be synchronized utilizing single-fluorochrome–conjugated  
409 surface-dyed beads for standardized immunophenotyping, *Clinical Laboratory Analysis*, 34, e23361,  
410 <https://doi.org/10.1002/jcla.23361>, 2020.
- 411 D’Amato, G., Cecchi, L., Bonini, S., Nunes, C., Annesi-Maesano, I., Behrendt, H., Liccardi, G., Popov, T.,  
412 and van Cauwenberge, P.: Allergenic pollen and pollen allergy in Europe, *Allergy*, 62, 976–990,  
413 <https://doi.org/10.1111/j.1398-9995.2007.01393.x>, 2007.
- 414 De Weger, L. A., Bergmann, K. Ch., Rantio-Lehtimäki, A., Dahl, A., Buters, J., Déchamp, C., Belmonte,  
415 J., Thibaudon, M., Cecchi, L., Besancenot, J.-P., Galán, C., and Waisel, Y.: Impact of Pollen, in: *Allergenic*  
416 *Pollen: A Review of the Production, Release, Distribution and Health Impacts*, 161,203, 2013.
- 417 De Weger, L. A., Verbeek, C., Markey, E., O’Connor, D. J., and Gosling, W. D.: Greater difference between  
418 airborne and flower pollen chemistry, than between pollen collected across a pollution gradient in the  
419 Netherlands, *Science of The Total Environment*, 934, 172963,  
420 <https://doi.org/10.1016/j.scitotenv.2024.172963>, 2024.
- 421 Donaldson, L.: Autofluorescence in Plants, *Molecules*, 25, 2393,  
422 <https://doi.org/10.3390/molecules25102393>, 2020.
- 423 Dunker, S., Boyd, M., Durka, W., Erler, S., Harpole, W. S., Henning, S., Herzsuh, U., Hornick, T., Knight,  
424 T., Lips, S., Mäder, P., Švara, E. M., Mozarowski, S., Rakosy, D., Römermann, C., Schmitt-Jansen, M.,  
425 Stooß-Leichsenring, K., Stratmann, F., Treudler, R., Virtanen, R., Wendt-Potthoff, K., and Wilhelm, C.:  
426 The potential of multispectral imaging flow cytometry for environmental monitoring, *Cytometry Pt A*, 101,  
427 782–799, <https://doi.org/10.1002/cyto.a.24658>, 2022.

- 428 Dunker, S., Motivans, E., Rakosy, D., Boho, D., Mäder, P., Hornick, T., and Knight, T. M.: Pollen analysis  
429 using multispectral imaging flow cytometry and deep learning, *New Phytologist*, 229, 593–606,  
430 <https://doi.org/10.1111/nph.16882>, 2021.
- 431 Erb, S., Graf, E., Zeder, Y., Lionetti, S., Berne, A., Clot, B., Lieberherr, G., Tummon, F., Wullschleger, P.,  
432 and Crouzy, B.: Real-time pollen identification using holographic imaging and fluorescence measurements,  
433 *Atmos. Meas. Tech.*, 17, 441–451, <https://doi.org/10.5194/amt-17-441-2024>, 2024.
- 434 Falagiani, P.: *Pollinosis*, CRC Press, 288 pp., 1989.
- 435 Gierlicka, I., Kasprzyk, I., and Wnuk, M.: Imaging Flow Cytometry as a Quick and Effective Identification  
436 Technique of Pollen Grains from Betulaceae, Oleaceae, Urticaceae and Asteraceae, *Cells*, 11, 598,  
437 <https://doi.org/10.3390/cells11040598>, 2022.
- 438 Grandini, M., Bagli, E., and Visani, G.: Metrics for Multi-Class Classification: an Overview,  
439 <https://doi.org/10.48550/arXiv.2008.05756>, 13 August 2020.
- 440 Hernández, J., Sucar, L. E., and Morales, E. F.: Multidimensional hierarchical classification, *Expert Systems*  
441 *with Applications*, 41, 7671–7677, <https://doi.org/10.1016/j.eswa.2014.05.054>, 2014.
- 442 Holt, K. A. and Bennett, K. D.: Principles and methods for automated palynology, *New Phytologist*, 203,  
443 735–742, <https://doi.org/10.1111/nph.12848>, 2014.
- 444 Kim, K. R., Oh, J.-W., Woo, S.-Y., Seo, Y. A., Choi, Y.-J., Kim, H. S., Lee, W. Y., and Kim, B.-J.: Does  
445 the increase in ambient CO<sub>2</sub> concentration elevate allergy risks posed by oak pollen?, *Int J Biometeorol*,  
446 62, 1587–1594, <https://doi.org/10.1007/s00484-018-1558-7>, 2018.
- 447 Konecny, A. J., Mage, P. L., Tyznik, A. J., Prlic, M., and Mair, F.: OMIP-102: 50-color phenotyping of the  
448 human immune system with in-depth assessment of T cells and dendritic cells, *Cytometry Part A*, 105,  
449 430–436, <https://doi.org/10.1002/cyto.a.24841>, 2024.
- 450 Ladeau, S. L. and Clark, J. S.: Pollen production by *Pinus taeda* growing in elevated atmospheric CO<sub>2</sub>,  
451 *Functional Ecology*, 20, 541–547, <https://doi.org/10.1111/j.1365-2435.2006.01133.x>, 2006.
- 452 Martin, A. C. and Harvey, W. J.: The Global Pollen Project: a new tool for pollen identification and the  
453 dissemination of physical reference collections, *Methods Ecol Evol*, 8, 892–897,  
454 <https://doi.org/10.1111/2041-210X.12752>, 2017.
- 455 Medek, D. E., Katelaris, C. H., Milic, A., Beggs, P. J., Lampugnani, E. R., Vicendese, D., Erbas, B., and  
456 Davies, J. M.: Aerobiology matters: Why people in the community access pollen information and how they  
457 use it, *Clinical & Translational All*, 15, e70031, <https://doi.org/10.1002/ct2.70031>, 2025.
- 458 Mousavi, F., Oteros, J., Shahali, Y., and Carinanos, P.: Impacts of climate change on allergenic pollen  
459 production: A systematic review and meta-analysis, *Agricultural and Forest Meteorology*, 349, 109948,  
460 <https://doi.org/10.1016/j.agrformet.2024.109948>, 2024.
- 461 Ogden, E. C., Museum, N. Y. S., Service, S., and Commission, U. S. A. E.: *Manual for Sampling Airborne*  
462 *Pollen*, Hafner Press, 1974.
- 463 Omana-Zapata, I., Mutschmann, C., Schmitz, J., Gibson, S., Judge, K., Aruda Indig, M., Lu, B., Taufman,  
464 D., Sanfilippo, A. M., Shallenberger, W., Graminske, S., McLean, R., Hsen, R. I., d’Empaire, N., Dean, K.,  
465 and O’Gorman, M.: Accurate and reproducible enumeration of T-, B-, and NK lymphocytes using the BD

- 466 FACSLyric 10-color system: A multisite clinical evaluation, *PLoS ONE*, 14, e0211207,  
467 <https://doi.org/10.1371/journal.pone.0211207>, 2019.
- 468 Paquette, A., Sousa-Silva, R., Fernandez, M., Faticov, M., Schillé, L., Bacon, E., Cameron, E., Fraysse, J.,  
469 gagnon Koudji, E., Poirier, S., Rondeau-Leclaire, J., Tardif, S., Handa, T., Laforest-Lapointe, I., Puric-  
470 Mladenovic, D., and Ziter, C.: Montreal Urban Observatory: research platform to monitor urban forest  
471 ecosystems for global change adaptation and health,  
472 <https://doi.org/https://doi.org/10.64898/2026.02.07.704556>, 2026.
- 473 Pöhlker, C., Huffman, J. A., Förster, J.-D., and Pöschl, U.: Autofluorescence of atmospheric bioaerosols:  
474 spectral fingerprints and taxonomic trends of pollen, *Atmos. Meas. Tech.*, 6, 3369–3392,  
475 <https://doi.org/10.5194/amt-6-3369-2013>, 2013.
- 476 Šaulienė, I., Šukienė, L., Daunys, G., Valiulis, G., Vaitkevičius, L., Matavulj, P., Brdar, S., Panic, M.,  
477 Sikoparija, B., Clot, B., Crouzy, B., and Sofiev, M.: Automatic pollen recognition with the Rapid-E particle  
478 counter: the first-level procedure, experience and next steps, *Atmos. Meas. Tech.*, 12, 3435–3452,  
479 <https://doi.org/10.5194/amt-12-3435-2019>, 2019.
- 480 Savouré, M., Bousquet, J., Jaakkola, J. J. K., Jaakkola, M. S., Jacquemin, B., and Nadif, R.: Worldwide  
481 prevalence of rhinitis in adults: A review of definitions and temporal evolution, *Clinical & Translational*  
482 *All*, 12, e12130, <https://doi.org/10.1002/ctt2.12130>, 2022.
- 483 Sikoparija, B., Matavulj, P., Simovic, I., Radisic, P., Brdar, S., Minic, V., Tesendic, D., Kadantsev, E.,  
484 Palamarchuk, J., and Sofiev, M.: Classification accuracy and compatibility across devices of a new Rapid-  
485 E+ flow cytometer, <https://doi.org/10.5194/egusphere-2024-187>, 2 April 2024.
- 486 Smith, E. G.: Sampling and identifying allergenic pollens and molds. An illustrated manual for physicians  
487 and lab technicians., *Sampling and identifying allergenic pollens and molds. An illustrated manual for*  
488 *physicians and lab technicians.*, 1984.
- 489 Solly, F., Rigollet, L., Baseggio, L., Guy, J., Borgeot, J., Guérin, E., Debliquis, A., Drenou, B., Campos, L.,  
490 Lacombe, F., and Béné, M. C.: Comparable flow cytometry data can be obtained with two types of  
491 instruments, Canto II, and Navios. A GEIL study, *Cytometry A*, 83, 1066–1072,  
492 <https://doi.org/10.1002/cyto.a.22404>, 2013.
- 493 Sousa-Silva, R., Smargiassi, A., Paquette, A., Kaiser, D., and Kneeshaw, D.: Exactly what do we know  
494 about tree pollen allergenicity?, *The Lancet Respiratory Medicine*, 8, e10, [https://doi.org/10.1016/S2213-2600\(19\)30472-2](https://doi.org/10.1016/S2213-2600(19)30472-2), 2020.
- 496 Steckling-Muschack, N., Mertes, H., Mittermeier, I., Schutzmeier, P., Becker, J., Bergmann, K.-C., Böse-  
497 O'Reilly, S., Buters, J., Damialis, A., Heinrich, J., Kabesch, M., Nowak, D., Walser-Reichenbach, S.,  
498 Weinberger, A., Zamfir, M., Herr, C., Kutzora, S., and Heinze, S.: A systematic review of threshold values  
499 of pollen concentrations for symptoms of allergy, *Aerobiologia*, 37, 395–424,  
500 <https://doi.org/10.1007/s10453-021-09709-4>, 2021.
- 501 Swanson, B., Freeman, M., Rezgui, S., and Huffman, J. A.: Pollen classification using a single particle  
502 fluorescence spectroscopy technique, *Aerosol Science and Technology*, 57, 112–133,  
503 <https://doi.org/10.1080/02786826.2022.2142510>, 2023.
- 504 Tardif, S.: Pollen Flow Cytometry Datasets and Classification Models. (v1),  
505 <https://doi.org/https://doi.org/10.6084/m9.figshare.30870641>, 2025.

506 Tummon, F., Adams-Groom, B., Antunes, C. M., Bruffaerts, N., Buters, J., Cariñanos, P., Celenk, S., Choël,  
507 M., Clot, B., Cristofori, A., Crouzy, B., Damialis, A., Fernández, A. R., González, D. F., Galán, C., Gedda,  
508 B., Gehrig, R., Gonzalez-Alonso, M., Gottardini, E., Gros-Daillon, J., Hajkova, L., O'Connor, D.,  
509 Östensson, P., Oteros, J., Pauling, A., Pérez-Badia, R., Rodinkova, V., Rodríguez-Rajo, F. J., Ribeiro, H.,  
510 Sauliene, I., Sikoparija, B., Skjøth, C. A., Spanu, A., Sofiev, M., Sozinova, O., Srnec, L., Visez, N., and De  
511 Weger, L. A.: The role of automatic pollen and fungal spore monitoring across major end-user domains,  
512 *Aerobiologia*, 40, 57–75, <https://doi.org/10.1007/s10453-024-09820-2>, 2024.

513 Wang, L. and Hoffman, R. A.: Standardization, Calibration, and Control in Flow Cytometry, *CP Cytometry*,  
514 79, <https://doi.org/10.1002/cpcy.14>, 2017.

515 Zhang, G. and Abdulla, W.: Identifying Pollen Species Using Multispectral Imaging Flow Cytometry and  
516 Neural Networks, <https://doi.org/10.2139/ssrn.4375939>, 2023.

517 Zhang, Y. and Steiner, A. L.: Projected climate-driven changes in pollen emission season length and  
518 magnitude over the continental United States, *Nat Commun*, 13, 1234, [https://doi.org/10.1038/s41467-022-](https://doi.org/10.1038/s41467-022-28764-0)  
519 [28764-0](https://doi.org/10.1038/s41467-022-28764-0), 2022.

520 Ziska, L. H., Makra, L., Harry, S. K., Bruffaerts, N., Hendrickx, M., Coates, F., Saarto, A., Thibaudon, M.,  
521 Oliver, G., Damialis, A., Charalampopoulos, A., Vokou, D., Heidmarsson, S., Guđjohnsen, E., Bonini, M.,  
522 Oh, J.-W., Sullivan, K., Ford, L., Brooks, G. D., Myszkowska, D., Severova, E., Gehrig, R., Ramón, G. D.,  
523 Beggs, P. J., Knowlton, K., and Crimmins, A. R.: Temperature-related changes in airborne allergenic pollen  
524 abundance and seasonality across the northern hemisphere: a retrospective data analysis, *The Lancet*  
525 *Planetary Health*, 3, e124–e131, [https://doi.org/10.1016/S2542-5196\(19\)30015-4](https://doi.org/10.1016/S2542-5196(19)30015-4), 2019.  
526